Large Propeptides of Fungal β-*N*-Acetylhexosaminidases Are Novel Enzyme Regulators That Must Be Intracellularly Processed to Control Activity, Dimerization, and Secretion into the Extracellular Environment†

Ondřej Plíhal,‡ Jan Sklenář,‡ Kateřina Hofbauerová,‡,|| Petr Novák,‡ Petr Man,‡ Petr Pompach,‡ Daniel Kavan,‡,§ Helena Ryšlavá,§ Lenka Weignerová,‡ Andrea Charvátová-Pišvejcová,‡ Vladimír Křen,‡ and Karel Bezouška*,‡,§

Institute of Microbiology, Academy of Sciences of the Czech Republic, Vídeňská 1083, 14220 Praha 4, Czech Republic, Department of Biochemistry, Faculty of Science, Charles University, Hlavova 8, 12840 Praha 2, Czech Republic, and Institute of Physics, Faculty of Mathematics and Physics, Charles University, Ke Karlovu 5, 12116 Praha 2, Czech Republic

Received September 1, 2006; Revised Manuscript Received December 22, 2006

ABSTRACT: Filamentous fungi produce and secrete β-*N*-acetylhexosaminidases, Hex, as important components of the binary chitinolytic systems involved in the formation of septa and hyphenation. Enzyme reconstitution experiments published previously indicate that Hex can occur in the form of two molecular species containing either one or two molecules of the propeptide noncovalently associated with the enzyme dimer. Here, we describe a novel mechanism for the regulation of the activity of Hex based on the association of their catalytic subunits with the large N-terminal propeptides *in vivo*. We show that the enzyme precursor is processed early in the biosynthesis, shortly after the addition of *N*-glycans through the action of a dibasic peptidase, cleaving both before and after the dibasic sequence. The processing site for this unique dibasic peptidase, different from that of kexins, is conserved among the β-*N*-acetylhexosaminidases from filamentous fungi, and inhibition of the dibasic peptidase abrogates enzyme folding and activation. Binding of the released propeptide to the catalytic subunit of Hex is essential for its activation. An examination of the kinetics of Hex activation and dimerization *in vitro* allowed us to understand the unusually high efficiency of the assembly of this enzyme. We also report that the fungus is able to actively regulate the concentration of the processed propeptide in endoplasmic reticulum and thus the specific activity of the produced Hex. This novel regulatory mechanism enables the control of the catalytic activity and architecture of the secreted enzyme according to the needs of the producing cell at various stages of its growth cycle.

β-*N*-Acetylhexosaminidases (Hex[1], EC 3.2.1.52) are exoglycosidases able to hydrolyze both β-linked GlcNAc and GalNAc residues (*1*). These enzymes are widely distributed in nature and are known to be responsible for a large variety of degradation processes. They have been extensively studied in higher vertebrates (including humans) and in bacteria. In humans, they are dimeric lysosomal enzymes composed of two subunits, α and β, having approximately 60% sequence identities (*2*, *3*). They occur in three isoforms, the homodimeric hexosaminidases B (ββ) and S (αα) and the heterodimeric hexosaminidase A (αβ). Dimerization is required for the catalytic activity of these enzymes. Interest in human hexosaminidases is connected with the allelic variations in the *HexA* and *HexB* genes that cause the fatal inborn errors of metabolism known as Tay-Sachs and Sandhoff disease, respectively. However, the amino acid residues involved in catalysis by these enzymes have been first identified in the bacterial enzyme from *Serratia marcescens* that could be easily prepared and crystallized (*4*).

Recently, β-*N*-acetylhexosaminidases from filamentous fungi have attracted considerable attention because of their importance in the biology of these organisms and their unique enzymatic properties. First, unlike the human and bacterial Hex's, which are lysosomal or membrane-associated, their fungal orthologues are robust enzymes that are extracellularly secreted and remain active in the oxidative extracellular environment (*5*, *6*). Second, these enzymes were shown to hydrolyze chitobiose as well as the higher chito-oligomers produced from cell wall chitin by endochitinases (*7*−*9*), thus contributing to the formation of septa during the hyphenation

† This work was supported by the Ministry of Education of the Czech Republic (MSM 21620808, MSM 21620835, LC545, LC06010), by the Institutional Research Concept for the Institute of Microbiology (AVOZ50200510), and by the Czech Science Foundation (grants 203/04/1045, 203/05/0172, 204/06/0771, and IAA5020403).

* To whom correspondence should be addressed. Phone: +420-2-4106-2142. Fax: +420-2-4106-2383. E-mail: bezouska@biomed.cas.cz.

‡ Academy of Sciences of the Czech Republic.

§ Department of Biochemistry, Charles University.

|| Institute of Physics, Charles University.

[1] Abbreviations: BCA, bicinchonic acid; CCF, Czech Collection of Fungi; CTP, cytidine triphosphate; CY, cytosol; EDC, 1′-ethyl-3′-dimethylaminopropylcarbodiimide hydrochloride; EDTA, ethylenediamine tetraacetic acid; EGTA, ethylene glycol tetraacetic acid; ER, endoplasmic reticulum; GADPH, glyceraldehyde phosphate dehydrogenase; Hex, hexosaminidase; MALDI, matrix-assisted laser desorption and ionization; MHC, major histocompatibility complex; MS, mass spectrometry; NAG-thiazoline, *N*-acetylglucosamine thiazoline; PBS, phosphate buffered saline; PMSF, phenyl methyl sulfonyl fluoride; PVDF, polyvinylidene difluoride; S.D., standard deviation; SSC, sodium salt citrate; TBS, Tris buffered saline, 10 mM Tris-HCl at pH 8.0 containing 150 mM NaCl; TFA, trifluoroacetic acid.

10.1021/bi061828m CCC: $37.00
Published on Web 02/16/2007

of the fungus. Third, the fungal Hex's are inducible both by their substrates and by the end products such as GlcNAc (*5*, *6*). We have previously described the inducibility of Hex secreted from the collection strain of *Aspergillus oryzae* CCF 1066 (*5*). The activity accumulated in the medium in two waves, the second of which occurred as late as on days 11−14 (*5*). Individual fungi secrete Hex's with characteristic enzymatic properties, which could be used for their taxonomy (*1*, *6*). Moreover, we have described the isolation and characterization of Hex from *A. oryzae* CCF 1066 (*10*). On the basis of the solved primary structure (GenBank accession number AY091636) and homology, a 3D model of the enzyme has been created and proved useful for the prediction of substrate specificity (*11*) and molecular analysis. We have also described the unique glycosylation of the above enzyme in which the processed O-glycosylated propeptide cooperates with the N-glycosylated catalytic unit to attain full enzymatic activity (*10*). Reconstitution studies *in vitro* indicated that Hex containing two moles of propeptide per dimer of catalytic subunits had 2-fold specific activity compared to that of the species composed of a single propeptide per dimer.

Here, we report that both the large N-terminal propeptides and the dibasic processing motifs at their C-termini are specific for Hex from filamentous fungi. Using Hex from *A. oryzae*, we obtained evidence that the enzyme precursor must be processed intracellularly in order for the propeptide to be able to associate noncovalently with the catalytic subunits and to control the activity, dimerization, and secretion of the enzyme. The processing occurs early in the biosynthesis by ER dibasic peptidase, distinct from the fungal Kex2. Association of the propeptide with the catalytic subunit is fast and specific and precedes enzyme dimerization. Either one or two molecules of the propeptide associated noncovalently with the dimer of the catalytical subunit, but the latter form of the enzyme is formed and secreted much faster. *A. oryzae* uses an active mechanism of propeptide depletion from ER in physiological situations when lower Hex activities in the medium are required. This provides a novel and straightforward mechanism for the functionally important regulation of Hex activity in the extracellular environment.

MATERIALS AND METHODS

Materials. The chloromethane tripeptides were synthesized as previously described (*12*). [^{35}S]-Translabel, a mixture of ^{35}S-cysteine and ^{35}S-methionine for protein labeling, was from ICN Biomedicals. All other chemicals were analytical grade reagents from Sigma.

Multiple Sequence Alignments and Construction of the Evolutionary Tree. For the initial screen of protein sequence similarity, the BLASTp algorithm (*13*) implemented at www.ncbi.nlm.nig.gov was used. For multiple sequence alignment of Hex sequences and the construction of a phylogenic tree, an algorithm based on a highly conserved motif in the catalytic domain was employed using the PAM 350 matrix with the CLUSTALX and TreeView programs (*11*).

Microbial Strains and Growth Conditions. Aspergillus oryzae strain CCF 1066 (Czech Collection of Fungi, Department of Botany, Charles University, Prague) was grown on a minimal medium consisting of 0.3% KH_2PO_4, 0.5% $NH_4H_2PO_4$, 0.2% $(NH_4)_2SO_4$, 1.5% NaCl, 0.05% $MgSO_4$, 0.05% yeast extract, and 0.5% *N*-acetyl-D-glucosamine at pH 6.0. The fungus was cultivated at 28 °C for the times indicated for the individual experiments. The mycelium used for the isolation of chromosomal DNA and biochemical studies was collected after 48−50 h unless otherwise indicated, and the medium for enzyme isolations was collected after 10 days.

Isolation of the Intracellular Enzyme. Purification of Hex from the medium is described in the Supporting Information. The mycelium was filtered, washed with 100 mL of cold distilled water, immediately frozen in the liquid nitrogen, and stored at −80 °C. The frozen mycelium was mixed with 5 mL of the detergent extraction buffer (50 mM citrate buffer at pH 5.0 containing 0.5 M $(NH_4)_2SO_4$, 1.0% octyl-β-glucoside, and 1 mM NaN_3) and sonicated for 6 × 1 min on ice. The extract was centrifuged at 20 000*g* for 30 min at 4 °C and used for the isolation of hexosaminidase as described in the Supporting Information. To resolve the Hex isoforms, the shallow gradient was used for the elution of the MonoQ column, increasing the NaCl concentration by 0.5 mmol/min.

Separation of the Propeptide from the Catalytic Unit. The propeptide was separated from the catalytic unit of Hex on a C4 column (4.6 × 250 mm, Vydac) using a linear gradient from 0 to 95% acetonitrile in 0.07% TFA over 60 min. The propeptide eluted from the column at approximately 41 min, while the catalytic unit eluted at approximately 47 min (*10*). Both polypeptides were collected into 0.2 mL fractions and analyzed by SDS electrophoresis, and the pure fractions were pooled and evaporated to dryness. Alternatively, a polymeric reverse phase separation column PLRP-S (4000 Å, 2.1 × 150 mm; Polymer Laboratories) has been employed under identical chromatographical conditions.

Production of Polyclonal Antibodies. Antibodies against both the catalytic unit and the propeptide of Hex were raised in rabbits using the standard immunization protocol (*14*) and purified using the respective protein antigens immobilized to CNBr-activated Sepharose 4B (GE Healthcare) as recommended by the manufacturer. The immunoabsorbed antibodies were eluted with 0.2 M glycine buffer at pH 2.5 directly into 1 M Tris-HCl at pH 8.0, dialyzed against PBS at pH 7.4, concentrated to 5 mg/mL, and stored in 1 mM NaN_3 at 4 °C.

SDS−PAGE and Western Blotting. SDS−PAGE and Western blotting were performed according to the standard protocols (*15*). Separated proteins were electrotransferred onto nitrocellulose membranes (BioTraceNT, Pall Corp., MI), and the membranes were blocked in PBS with 2% BSA, incubated in primary antibodies (0.1 mg/mL in PBS with 2% BSA), washed 3 × 10 min in PBS, and developed using secondary antibodies (goat anti-rabbit) conjugated with horseradish peroxidase and ECL (GE Healthcare).

Cross-Linking Experiments. Hex (25 μg) was transferred into 200 μL of 0.1 M MES buffer at pH 5.0 containing 0.1 M NaCl using Centricon 30 (Millipore). 1′-Ethyl-3′-dimethylaminopropylcarbodiimide hydrochloride (EDC) was added to a final concentration of 10 mM, and the reaction proceeded for 2 h at room temperature (*16*). Triton X-100 was added to 0.5% (v/v), and the sample was precipitated with 10% trichloroacetic acid, washed twice with 500 μL of ethanol/ether (1:1, v/v), and dried. The sample was dissolved in sample buffer containing 100 mM DTT, and the proteins

were separated in 8% polyacrylamide gels. Gels were stained with Coomassie Brilliant Blue R-250. The control experiment was performed under identical conditions in the presence of a 10 mM glycine quencher in the reaction buffer.

Reconstitution Experiments. Propeptide was separated from the catalytic unit as described above, and both components were transferred to 0.1% TFA and 20% acetonitrile using 1 mL spin columns packed with Sephadex G-25. In a standard reconstitution experiment, 1 nmol of the purified catalytic subunit in 10 μL of the above solvent was mixed with 990 μL of the enzyme stabilization buffer (50 mM citrate buffer at pH 5.0 with 0.5 M $(NH_4)_2SO_4$ and 1 mM NaN_3), containing varying amounts (0.5 nmol; 1 nmol) of the propeptide, and incubated for 1 h at room temperature. Alternatively, 10 μL of propeptide solution was added to 1 nmol of the catalytic unit diluted as above and incubated for an additional 1 h at room temperature. The mixture was used for the determination of protein concentrations and the enzymatic activity and for rapid gel filtration (TSK G3000SW precolumn from GE Healthcare eluted in enzyme stabilization buffer at 1 mL/min) after concentration to 100 μL using Centricon 30 (Millipore).

Synthesis and Evaluation of the NAG-Thiazoline Inhibitor. The NAG-thiazoline inhibitor was synthesized according to the published procedure (*17*). The structure of the final compounds was verified by ^{1}H and ^{13}C NMR spectroscopy using a Varian INOVA-400 spectrometer at 399.89 and 100.55 MHz, respectively, on the basis of gCOSY, HMQC, and 1D-TOCSY experiments. The type of inhibiton and K_i values were determined using the standard enzymology procedures (*17*). The rate of dissociation of the inhibitor from the enzyme was measured after 10 min of incubation in the presence of 10 mM inhibitor by removing the inhibitor using the spin column technique (*16*) with dried Sephadex G25 and assaying the activity of Hex against the control without inhibitor preincubation. To evaluate *in vivo* activities of the inhibitor, the culture of *A. oryzae* was grown in shaker flasks, and the total activity of the intracellular enzyme was determined in 2 min intervals after the addition of the inhibitor as described in the following paragraph. To follow the Hex activity after the withdrawal of the NAG-thiazoline inhibitor, cultures were incubated in the presence of 10 mM inhibitor for 10 min, the fungi were filtered, transferred to a fresh medium, and incubated for 10 min, and thereafter, enzyme activity was assayed in 2 min intervals as described below.

Pulse−Chase Labeling Experiments. The culture of *A. oryzae* was grown in a flask containing 200 mL of medium for 48 h under standard conditions. The mycelium was filtered, and the medium was saved. The mycelium was transferred into 100 mL of the filtered medium and pulsed for 1 min with [^{35}S]-Translabel (100 μCi). The mycelium was filtered, resuspended in the second portion (100 mL) of the label-free filtered medium, and chased for additional periods of time. Ten milliliter aliquots were withdrawn in 2 min intervals, and the mycelium was rapidly (10 s) filtered and immediately frozen in liquid nitrogen. In a second experiment, the fungus was cultivated in two flasks containing 200 mL of medium. Thirty minutes before the end of the 48 h incubation period, the mycelium in the first flask was incubated for 10 min in the presence of 10 mM NAG-thiazoline inhibitor. (This inhibitor concentration resulted in 98% inhibition of intracellular hexosaminidase as proved in preliminary experiments.) The mycelium was filtered, transferred to an inhibitor-free medium from the second flask (the mycelium from this flask was discarded), and then incubated for an additional 10 min to remove the inhibitor. Thereafter, the pulse−chase experiment was performed as described above. The intracellular β-*N*-acetylhexosaminidase was extracted as described above using 1 mL of extraction buffer. The extract was incubated with 100 μL of a 50% suspension of Sepharose beads containing the immobilized rabbit antibodies against the catalytic subunit of hexosaminidase equilibrated in the extraction buffer. The mixture was incubated overnight at 4 °C and washed five times with 1 mL of TBS. The enzyme was eluted from the immunoaffinity sorbent by 1 mL of 4 M $MgCl_2$ in TBS. This solution (0.75 mL) was concentrated to 30 μL in the enzyme stabilization buffer (see above) using a Microcon device (Millipore), and 10 μL aliquots were used for SDS electrophoresis, native electrophoresis, and the determination of enzymatic activity. The hexosaminidase (0.25 mL) eluted from the immunoaffinity column was incubated with 0.05 mL of a 50% suspension of concanavalin A−Sepharose beads (Amersham Biosciences), washed five times with 1 mL of TBS, and eluted with 0.25 mL of TBS containing 0.5 M D-glucose, concentrated to 10 μL in the enzyme stabilization buffer, and used for SDS electrophoresis. Proteins separated either by SDS electrophoresis or by native electrophoresis were fixed in 35% ethanol and 10% acetic acid, and the fixed gels were visualized by fluorography (Amplify, GE Healthcare).

Inhibition of Hex Processing in vivo. The pulse−chase experiment was performed essentially as described above in the presence of the indicated concentrations of the inhibitors. After SDS electrophoresis and fluorography, the processing of Hex at an individual time point was estimated from the densitometric evaluation of the fluorograms. From these data, the rate of processing in the presence of inhibitors was estimated and related to the rate of processing of uninhibited controls.

Isolation of the Unprocessed Intracellular Hex Using Double Immunoaffinity Purification. The mycelium from a large-scale (4 L) cultivation was extracted as described above using the detergent-containing buffer, and Hex was immunopurified using rabbit antibodies against the catalytic subunit as described above. The immunopurified Hex was subsequently immunoabsorbed onto the affinity matrix containing the rabbit antibodies against the propeptide immobilized onto CNBr-activated Sepharose 4B. The absorbed Hex was eluted by a stepwise acidic elution using 0.05 M citrate buffer at pH 4.5 to elute the unprocessed Hex followed by elution with 0.05 M citrate buffer at pH 3.5 to elute the processed Hex. The eluted unprocessed Hex was concentrated to 1 mg/mL in the stabilization buffer containing 0.5 M $(NH_4)_2SO_4$ and stored at 4 °C.

Determination of the Rate of Hex Processing in Vitro. Microsomal membrane fractions and cytosol were prepared from 500 mL cultures of *A. oryzae* (*18*), and frozen Microsomes were dissolved in 500 μL of the detergent containing Hex extraction buffer and clarified by centrifugation at 100 000*g* for 60 min. Then 90 μg of the immunopurified unprocessed Hex was mixed with 10 μL of the microsomal lysate and incubated at 18 °C. Ten microliter

aliquots were withdrawn at regular 2 min intervals and used for immunoblot assays, using polyclonal antibody against the catalytic subunit, and for Hex activity assays. In order to monitor the effects of protease inhibitors, individual compounds were added at the indicated concentrations, and the degree of conversion was determined from the immunoblot after 32 min of incubation.

Determination of the Rate of Hex Production and Secretion. After an appropriate period of cultivation, *A. oryzae* cultures were pulsed and chased as described above, except that samples of both the mycelium and the medium were collected in 5 min intervals. The mycelium was extracted as described above using the detergent-containing buffer, and the Hex contained in the mycelium and in the medium was immunopurified and the radioactivity determined by liquid scintillation counting. In order to calculate the weight amount of the produced and secreted Hex, the protein contents and the radioactivity of three isolated Hex protein bands were estimated by quantitative amino acid analysis and liquid scintillation counting, respectively.

Determination of Hex-Bound and Free Propeptide in the Microsomes and Cytosol. Microsomal membranes prepared from 500 mL cultures as described above were extracted in the extraction buffer used for the isolation of intracellular Hex, and the Hex-bound and free propeptide was obtained using consequtive immunopurifications on the antibodies against the catalytic subunit and the propeptide, respectively, immobilized onto CNBr-activated Sepharose (1 mg of antibodies/0.1 mL of beads). The bound proteins were eluted with 0.2 M glycine buffer at pH 3.5, and the propeptide was separated from the catalytic unit and analyzed as described above using HPLC on Vydac C4 columns and quantitative amino acid analysis of the separated fractions.

Other Analytical Techniques. The enzymatic activity was monitored using the chromogenic substrate 4-nitrophenyl-β-D-*N*-acetylglucosaminide and either the end-point (*19*) or kinetic (*20*) determination. The total protein was determined using the BCA assay (Sigma). Quantitative amino acid analysis was performed using AccuTag Kit (Waters). Blue native electrophoresis was performed as described in ref 21 (*21*). Proteins in the native electrophoresis strips were separated in the second (orthogonal) dimension by SDS−PAGE. Detection of activity in the native polyacrylamide gels was done by soaking the gel in 5 mM substrate for 5 min, developing in 1 M sodium carbonate, and immediately photographing the yellow stains. For the Northern blot analysis, total RNA were extracted from the crushed powder of mycelia as described in ref 9 (*9*). Ten micrograms of total RNA was analyzed by Northern blot analysis according to a standard method (*15*). The RNA was resolved by gel electrophoresis and transferred to a nitrocellulose membrane. The membrane was prehybridized in hybridization solution (50% formamide, 6× SSC, 5× Denhardt's, 1% SDS, and 50 μg/mL salmon sperm DNA (*15*)), hybridized with the probe overnight at 42 °C, washed in 0.25× SSC, 0.1% SDS at 42 °C, dried, and developed by autoradiography. The probes consisted of cDNA for the Hex of *A. oryzae* and GADPH that were labeled using a-[^{32}P]-CTP (3000 Ci/mmol) and the Random Hexanucleotide Primer Lableing Kit (both from GE Healthcare).

RESULTS

Existence of Large Propeptides Is Unique for the Subfamily of Fungal Hexosaminidases. We have previously reported the cloning and sequencing of β-*N*-acetylhexosaminidase from a filamentous fungus *A. oryzae* (see Supporting Information for the details of isolation, cloning, and sequencing), which has been shown to contain a signal peptide, an unusually large (78 amino acids) propeptide, and the catalytic subunit belonging to family 20 of the glycosylhydrolases (*10*). Multiple sequence alignment of our amino acid sequence against the protein sequence database using the standard BLAST-P program revealed four different categories of similarities based on the score value (Figure 1A). Only hexosaminidases from *A. oryzae* are similar (identical) over the entire sequence when compared against both the available parts of the incomplete sequence from another group (accession number AB085840) as well as against the conceptual translations from the completed genome sequence of *A. oryzae* (*22*). The second category is represented by eight cloned hexosaminidases from other filamentous fungi (score values from 944 to 739) that are available in the database (Figure 1A). The next most related group is represented by four cloned hexosaminidases from yeast (score from 540 to 517). Both latter groups display no similarity in the sequence of the signal peptide but are still very conserved in the region coding for the propeptide and the catalytic subunit. The fourth similarity category is represented by all the other hexosaminidases (score starting 371), of which only the five most similar sequences are presented in Figure 1A, but which follow the general evolutionary tree of all hexosaminidases (Figure 1B).

Although both filamentous fungi and the yeast have a sequence coding for the large, conserved propeptide in their genes, the detailed examination of these sequences (Figure 1C) revealed a principal difference between the two groups. In all hexosaminidases from the filamentous fungi, there is a dibasic KR processing motif for Kex2 proteases exactly at the border between the propeptide and the catalytic unit suggested by multiple sequence alignments (there are two such motifs in the *A. oryzae* hexosaminidase; cf. Figure 1C). This principal difference, together with a total lack of similarity with the nonfungal enzymes, suggests important dissimilarities in the biochemistry of the three major classes of hexosaminidases (i.e., those from the filamentous fungi, the yeasts, and all other organisms).

Processing and Activation of Hexosaminidase Occurs Intracellularly but the Propeptide Remains Noncovalently Bound to the Catalytic Unit. We (*10*) and others (*23*) have previously found that the dibasic KR processing motif at the end of the propeptide sequence is used as the processing site in the fungal hexosaminidases from *A. oryzae* and *P. chrysogenum*, respectively. In order to further clarify the occurrence of the putative propeptide in Hex, we perfomed additional analyses of the enzyme proteins from the former fungus. Gel filtration and native electrophoresis of Hex revealed its native molecular size of 160 kDa and suggested an oligomeric arrangement of the enzyme. However, this size was difficult to reconcile with the size of the 65 kDa catalytic unit observed on SDS electrophoresis (Figure 2A, lanes 1 and 3). The clarification of this discrepancy came from the occurrence of the processed propeptide, which could be

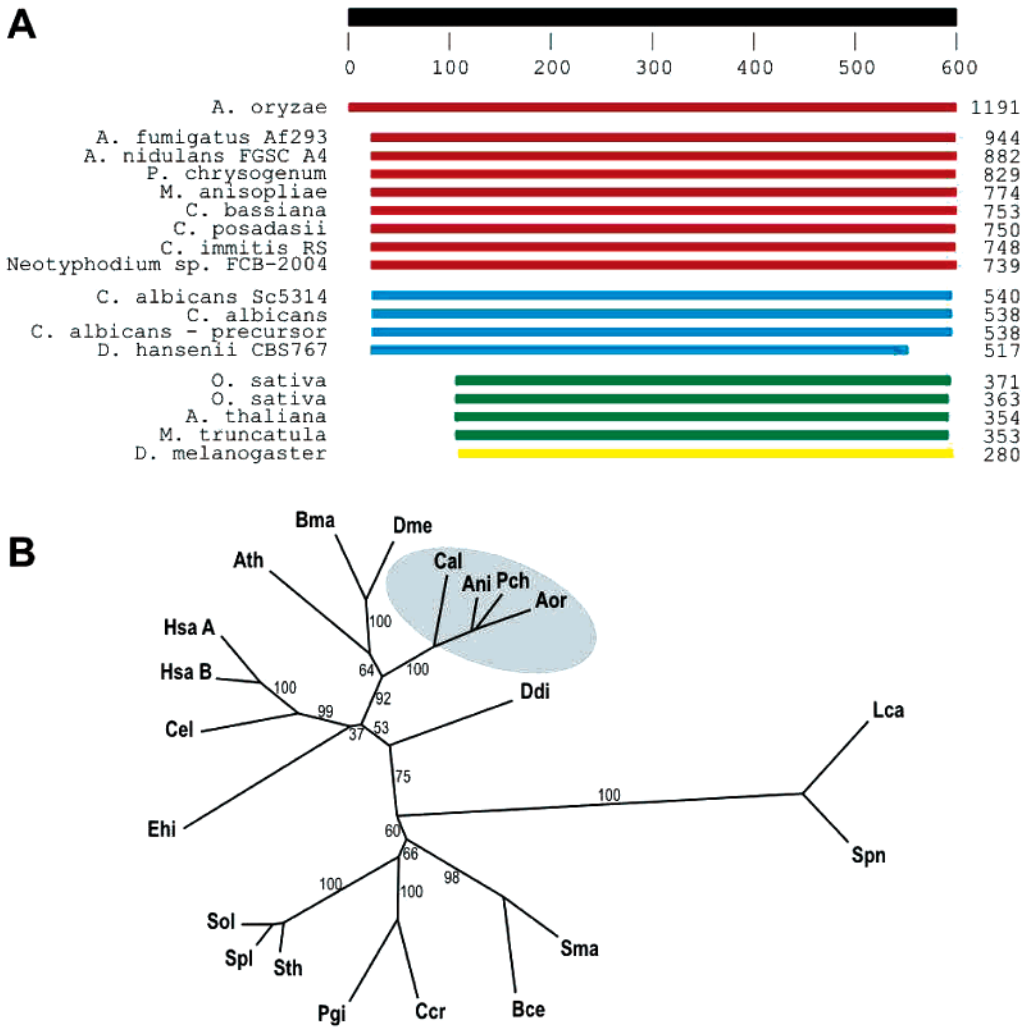

FIGURE 1: Sequence alignment and evolutionary tree of *β-N*-acetylhexosaminidase from *Aspergillus oryzae*. (A) Hexosaminidases with the highest alignment scores are produced in filamentous fungi (red), yeasts (blue), plants (green), and insects (yellow). The alignment scores are indicated on the right. (B) Phylogenetic tree of *β-N*-acetylhexosaminidases based on the sequence alignment of a highly conserved motif in the catalytic domain using the PAM 350 matrix with CLUSTALX and TreeView programmes. Abbreviations and GenBank accession numbers are as follows: *Arabidopsis thaliana* (Ath; AC007153), *Aspergillus nidulans* (Ani; AB039846), *Aspergillus oryzae* (Aor; AY091636), *Bombyx mandarina* (Bma; AF326597), *Burkholderia cepacia* (Bce; AB053088), *Caenorhabditis elegans* (Cel; U50199), *Candida albicans* (Cal; L26488), *Caulobacter crescentus* (Ccr; AE005718), *Dictyostelium discoideum* (Ddi; J04065), *Drosophila melanogaster* (Dme; AE003480), *Entamoeba histolytica* (Ehi; U09735), *Homo sapiens* (Hsa A; M13520; subunit A), *Homo sapiens* (Hsa B; M34906; subunit B), *Lactobacillus casei* (Lca; AB025100), *Penicillium chrysogenum* (Pch; AF056977), *Porphyromonas gingivalis* (Pgi; X78979), *Serratia marcescens* (Sma; L43594), *Streptococcus pneumoniae* (Spn; L36923), *Streptomyces olivaceoviridis* (Sol; AJ310133), *Streptomyces plicatus* (Spl; AF063001), and *Streptomyces thermoviolaceus* (Sth; AB015350). The most important bootstrap values are shown; the group of neighboring fungal/yeast *β-N*-acetylhexosaminidases, whose sequence alignment is shown in (C), is shaded. (C) Sequence alignment of four enzymes from fungi (*Aspergillus oryzae*, *Emericella nidulans*, and *Penicillium chrysogenum*) and yeast (*Candida albicans*). The chemical nature of the individual amino acids is color-coded as follows: cyan, W,F,V,Y,L,I,H,M,A; orange, G; yellow, P; magenta, D,E; green, N,S,T,Q; red, R,K; and pink, C. The KR dibasic processing sequence is indicated by a square.

detected as a diffuse band moving around 14 kDa that corresponded to the calculated mass of the propeptide together with O-glycosylation (ref 10 (*10*) and Figure 2A, lanes 1 and 4). When we performed 10 cycles of automated Edman degradation on the 14 kDa protein electrotransferred onto PVDF membrane, the N-terminal sequence was VGVN-PLPAPR, corresponding to the N-terminal sequence of the putative propeptide. However, the N-terminal sequencing of the 65 kDa band was ASNSLQYVNV, corresponding to the processed catalytic subunit. When we analyzed the enzyme under nonreducing conditions, the results were identical (Figure 2A, lane 2), indicating that unlike in the human Hex

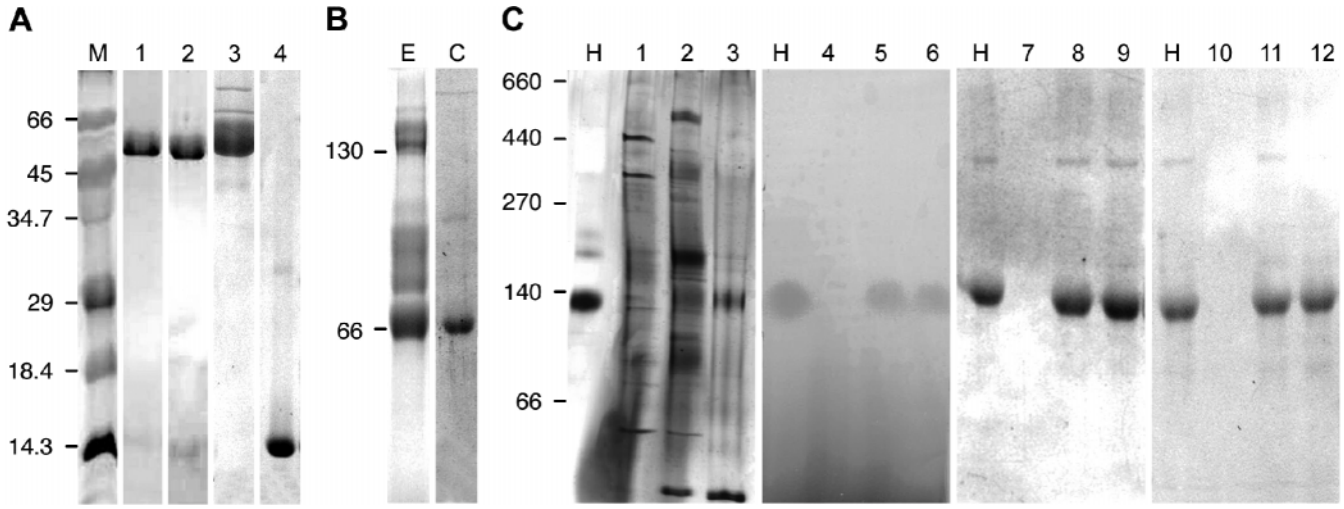

FIGURE 2: Electrophoretic characterization of Hex from *A.oryzae*. (A) Enzyme in 15% SDS polyacrylamide gel under reducing (lane 1) and nonreducing (lane 2) conditions stained with Coomassie Brilliant Blue R-250; lanes 3 and 4 are Hex separated under reducing conditions and immunoblotted by polyclonal antibody against the catalytic subunit and the propeptide, respectively; M is the molecular mass marker. (B) Enzyme from *A. oryzae* after EDC cross-linking (E) and analysis in 8% polyacrylamide gel compared to Hex cross-linked in the presence of a glycine quencher (C). (C) Examination of the *A. oryzae* proteome by native polyacrylamide gel electrophoresis stained for total protein (lanes 1−3), enzymatic activity (lanes 4−6), immunostained for the catalytic subunit (lanes 7−9), and immunostained for the propeptide (lanes 10−12). The proteome of the mycelium was examined after 12 h (lanes 1, 4, 7, and 10) and 48 h (lanes 2, 5, 8, and 11), together with the proteome of the medium after 48 h of cultivation (lanes 3, 6, 9, and 12); H is a marker of purified *A. oryzae* β-*N*-acetylhexosaminidase.

(*24*), the fungal enzymes do not contain a propeptide covalently bound through the disulfide bonds.

The purified propeptide was subjected to a detailed analysis by mass spectrometry in order to confirm its composition. Peptide fragments from tryptic digests of the propeptide analyzed by MALDI MS covered the propeptide sequence from Val^{19} to Ser^{96}. To further confirm our findings, the intact propeptide was analyzed using Fourier transformed mass spectrometry. Several unique masses differing by 162.053 mass units were observed. However, they fitted well the Val^{19}−Ser^{96} sequence with the different extent of O-glycosylation within the mass error 1.5 ppm (Pompach, P., Man, P., Novák, P., Kmoníčková, J., Plíhal, O., and Bezouška, K., unpublished experiments). Thus, the processing of the propeptide involved the elimination of the pentapeptide Lys^{97}-Lys-Ser-Lys-Arg^{101} at both the indicated dibasic peptide sequences. Moreover, these data clearly show that the dibasic processing peptidase cut both before and after the two dibasic sites, indicating rather unique specificity for the processing peptidase. Furthermore, we did not observe any additional degradation of the two polypeptides over the indicated processing sites.

The native molecular size of Hex (160 kDa) detected by gel filtration as well as by native electrophoresis (see below) could be most easily interpreted on the basis of the assumption that it contained two molecules of the 65 kDa catalytic units together with two molecules of the propeptide. In order to confirm such an arrangement, we employed cross-linking reagents and SDS electrophoresis of the reacted protein products. No cross-linked proteins could be detected using several homo and heterobifunctional reagents as well as a trifunctional reagent. However, the use of EDC, a simple condensation reagent and zero-length cross-linker, resulted in the formation of several compact protein bands that could be seen under experimental (Figure 2B, lane E) but not under control (Figure 2B, lane C) conditions. These corresponded to the isolated 65 kDa catalytic subunit, the subunit linked to one or two molecules of the propeptide, followed by the 130 kDa dimer of the catalytic subunit. The dimer linked to one or two molecules of the propeptide could also be observed as minor species at 145 and 160 kDa. However, essentially no species corresponding to higher oligomers were found.

In order to initiate the studies of *in vivo* Hex processing, we decided to compare the structure of the secreted form of the enzyme with the corresponding intracellular form. We monitored the time course for the occurrence of both forms of the enzyme using blue native electrophoresis and found a significant activity in the mycelium after 48 h of cultivation (Figure 2C, lanes 2 and 5) but not after 12 h of cultivation (Figure 2C, lanes 1 and 4). Similarly, significant activity of the enzyme secreted into the medium could be recorded only after 48 h of cultivation (Figure 2C, lanes 3 and 6). The native electrophoresis also confirmed that the intracellular form of the enzyme was indistinguishable from the one recovered from the medium: both forms of the enzyme contained the 65 kDa catalytic subunits noncovalently associated with the 14 kDa propeptide as documented by Western blotting of the electrophoreograms using antibodies specific against the catalytic unit (Figure 2C, lanes 8 and 9) and the propeptide (Figure 2C, lanes 11 and 12). These results allowed us to establish that at least 48 h of cultivation are required to stabilize the production of the enzyme and proved that Hex was processed intracellularly, most probably soon after the biosynthesis.

Unusual Properties of the NAG-Thiazoline Inhibitor. In order to trace the intracellular Hex and its activation, it would be an advantage to make use of the specific inhibitor of the enzyme. We used the NAG-thiazoline inhibitor that has been reported previously (*17*) to behave as a very efficient (K_i = 0.28 μM) competitive inhibitor of Hex from jack bean on the basis of its structural analogy with the transition state of

the substrate. However, the effect of NAG-thiazoline on Hex from *A.oryzae* studied here was different. The double reciprocal plot shown in Figure 3A clearly indicates that NAG-thiazoline behaved as a noncompetitive inhibitor, binding to both the free enzyme and the enzyme−substrate complex with $K_i = 70\ \mu M$. Although this value would make the NAG-thiazoline a rather inefficient inhibitor, we have shown that its dissociation from the enzyme molecule is rather slow, and after 30 min of incubation of the enzyme in the absence of NAG-thiazoline, less than 10% of the original activity is restored (Figure 3B).

In order to evaluate the use of the NAG-thiazoline inhibitor for *in vivo* tracing of the formation of Hex activity inside the fungus, we measured the effects of the addition and withdrawal of the inhibitor on the intracellular activity of Hex. Efficient inhibition of the intracellular Hex occurred within 2 min after the addition of an inhibitor (Figure 3C). However, after the withdrawal of the inhibitor, intracellular activity of Hex was restored much faster than it would correspond to mere inhibitor dissociation from the enzyme (Figure 3D): whereas less than 10% of the original activity of Hex was restored 30 min after inhibitor withdrawal *in vitro* (Figure 3B), the intracellular Hex activity in the growing fungus was efficiently and completely restored after about 10 min (Figure 3D). This fast reappearance of Hex activity was due to the *de novo* biosynthesis as detailed below.

Processing of the Propeptide Occurs in the Endoplasmic Reticulum by a Dibasic Peptidase Different from Kex2. To trace further the nature of the intracellular processing of the enzyme, we used 48 h cultures for pulse−chase labeling experiments. Because we wanted to observe not only the molecular forms of the enzyme but also the time of appearance of the enzymatic activity, we first inhibited all of the enzyme already present in the organism using the NAG-thiazoline inhibitor as described above. Twenty minutes of incubation in the presence of 10 mM NAG-thiazoline caused efficient inhibition of the activity of the intracellular enzyme, and after washing off the inhibitor, the time scale of the appearance of enzymatic activity could be monitored. When we performed a 1 min pulse with the ^{35}S-cysteine/methionine label followed by Hex immunopurification and measured the appearance of the freshly secreted enzyme in the medium, we found that the enzyme began to appear extracellularly only after an approximately 20 min lag period (see the last section of Results). Therefore, we investigated the molecular forms of intracellular Hex after the radioactive pulse within this time frame. The label appeared after 2 min in the nonglycosylated enzyme precursor that became fully N-glycosylated after 6 min as documented by concanavalin A binding (Figure 4A and B). The processed, and N-glycosylated polypeptide could be first observed after 8 min, and the enzyme was fully processed after 10 min (Figure 4A). The appearance of the enzymatic activity closely paralleled the processing of the enzyme. It began to be detectable after 8 min and was nearly fully established after 10 min (Figure 4C). The enzymatically active subunits started to dimerize as shown by native electrophoresis (Figure 4D). However, the dimerization appeared to be the rate-limiting process, and most of the enzyme was dimeric only 14 min after the pulse, shortly before the beginning of the intracellular transport and secretion.

In order to further investigate the requirement for the processing of the propeptide, we performed similar pulse−chase experiments in the presence of two protease inhibitors: leupeptine, a broad-range inhibitor of proteases active against serine- and cysteine-type proteases, and chloromethane tripeptides, which are the specific inhibitors of the serine-type dibasic peptidase (*25*). First, in order to exclude a possibility that the two inhibitors would exert nonspecific effects on the proteosynthesis, protein transport into ER, or protein stability within ER, we followed the time scale of protein occurrence using the ^{35}S-pulse−chase protocol. The radioactively labeled proteins occurred within the ER in 2 to 4 min (Figure 5A and B). Most importantly, however, there has been no effect of either of the protease inhibitor on the ER proteome when compared to the proteome of the untreated cells (Figure 5A and B, lane C). The processing and activation of Hex was then followed. In the presence of leupeptine, the rate of processing of the enzyme as well as the activation of the enzyme was only moderately delayed (Figure 5B and C). However, essentially no processing of the enzyme occurred in the presence of the specific dibasic protease inhibitor. Under these conditions, a rapid degradation of the unprocessed enzyme molecules was evident, and no enzymatic activity could be detected in the immunopurified material (Figure 5E and F).

We attempted to estimate the nature of the dibasic peptidase involved in Hex processing. The most common proprotein converting dibasic peptidases in fungi are the Kex2-like enzymes (kexins) that have been shown to be involved in the processing of a number of recombinant proteins produced in these organisms (*18*). However, the dibasic peptidase involved in the processing of Hex propeptide seems to be different from kexins. First, on the basis of the time course of Hex processing, the peptidase cleaving this enzyme shortly after its N-glycosylation seems to be localized in the endoplasmic reticulum, whereas Kex2 has been shown to localize in trans-Golgi and secretory vesicles (*26*). Second, as described above, all described Kex2-like dibasic peptidases cleave after the basic residues, whereas the Hex-processing peptidase must cleave both before and after these residues. Third, the effects of various inhibitors on Hex-processing peptidase when examined both *in vivo* and *in vitro* were clearly different from the effect of these compounds on other propeptide-converting peptidases such as Kex1p from *Saccharomyces cerevisiae* (*27*), krp from *Schizosaccharomyces* pombe (*28*), proinsulin-processing endopeptidase from rats (*25*), and prohormone convertase 5 (PC5) from rats (*29*). Hex-processing peptidase shared some similar features with the other propeptide-processing enzymes in that it was not inhibited by PMSF, 1,10-phenantroline, vanadate, and NaF and was sensitive to a partial inhibition by leupeptine and dibasic peptide inhibitors (Table 1). However, Hex-processing peptidase was sensitive to inhibition by sulfhydryl reagents such as iodoacetic acid, iodoacetamide, and *N*-ethylmaleiimide, whereas the other enzymes were not. Moreover, although all the other propeptide-converting enzymes were sensitive to $ZnCl_2$ and $HgCl_2$, Hex-processing peptidases retain full activity in the presence of these reagents both *in vivo* and *in vitro*. (EDTA and EGTA inhibition data remain controversial (Table 1).)

In order to further study the process of intracellular enzyme assembly, we used 48 h cultures from which we isolated

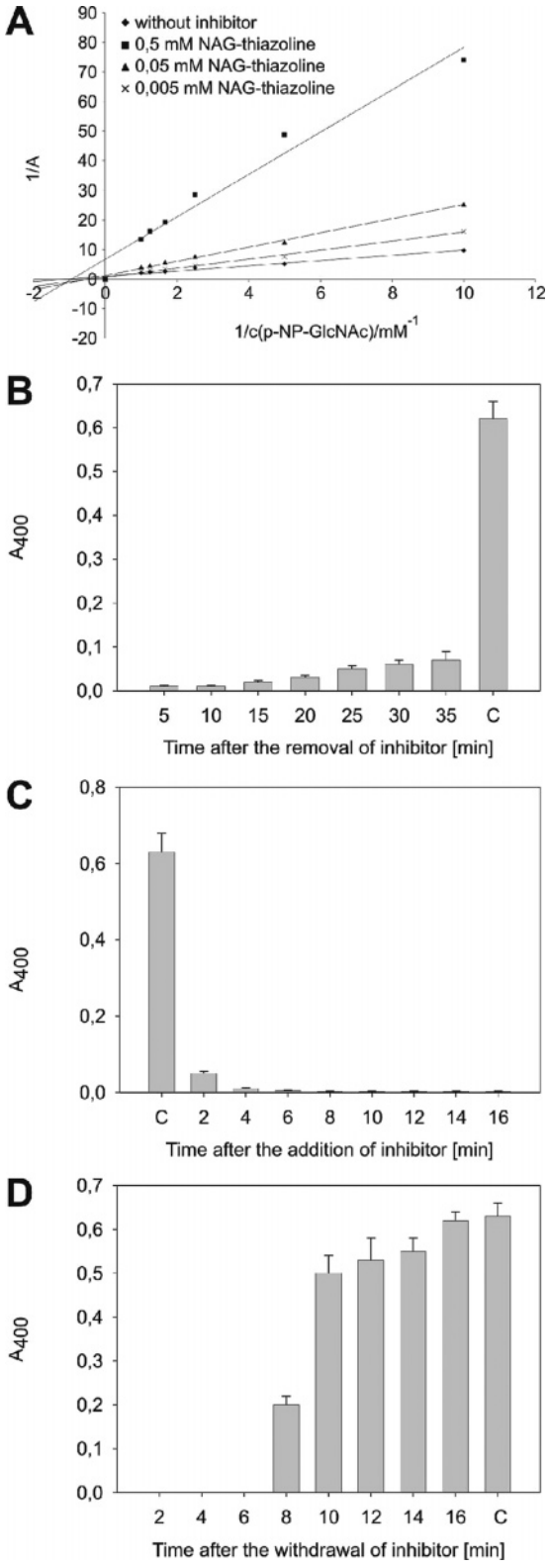

FIGURE 3: Evaluation of the inhibitory properties and *in vivo* accessibility of the NAG-thiazoline inhibitor. (A) Double reciprocal plot according to Lineweaver and Burk indicating the noncompetivite type of inhibition with $K_i = 70\ \mu$M. (B) Reactivation of Hex after the removal of the inhibitor by a spin column technique. C indicates the activity of the noninhibited control. (C) Effect of 10 mM NAG-inhibitor on intracellular Hex activity compared to that of the noninhibited control (C). (D) Restoration of the intracellular Hex activity after the withdrawal of the inhibitor compared to that of the noninhibited control (C). The bars in panels B−D indicate average values ± S.D. from three parallel determinations.

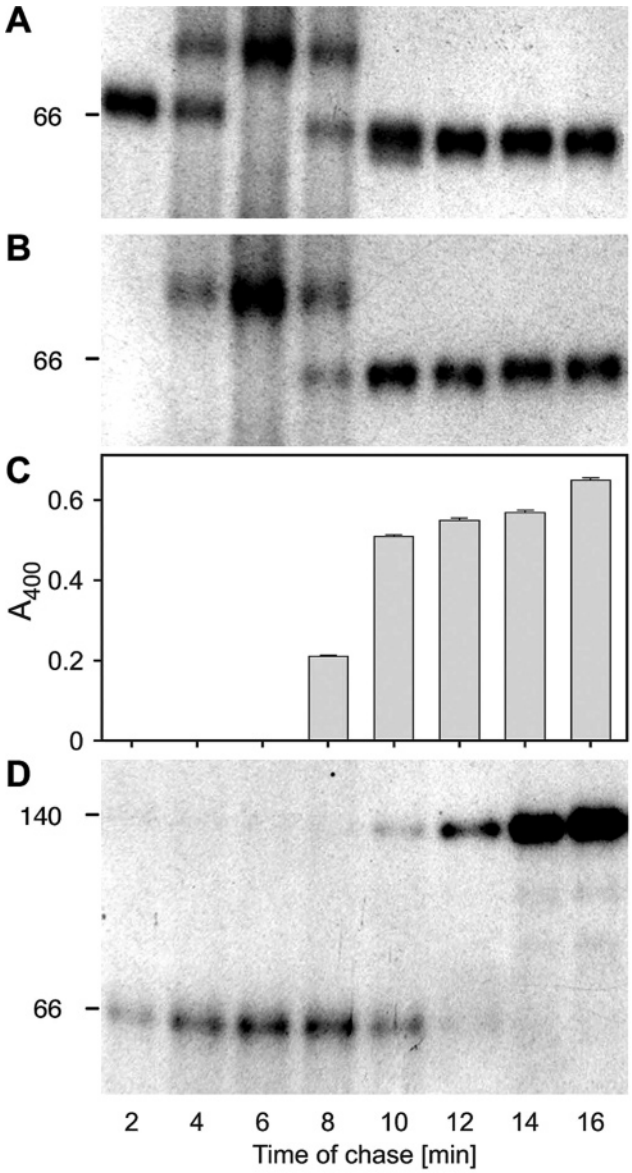

FIGURE 4: Analysis of the biosynthesis and activation of *A. oryzae* *β*-*N*-acetylhexosaminidase by pulse−chase labeling experiments. Samples were collected every 2 min and processed as described in Materials and Methods. (A) Analysis of ^{35}S-labeled protein by fluorography. (B) Analysis of N-glycosylation after concanavalin A purification. (C) Appearance of enzymatic activity measured by the colorimetric assays. (D) Analysis of enzyme dimerization using native electrophoresis. Molecular mass markers are indicated on the left sides of the panels.

the intracellular Hex and compared it with the secreted form of the enzyme. When we purified the secreted enzyme on a MonoQ column eluted with a slow salt gradient, the enzyme eluted in two peaks (Figure 6A). The enzyme eluted in the minor peak and the one found in the major peak were both dimeric (Figure 6B and C, respectively). However, the specific activity of the enzyme in the minor peak was only half of that recorded for the enzyme in the major peak (Figure 6B and C, respectively). Finally, reverse phase separations of enzymes in both peaks showed that the relative content of propeptide in the major peak was twice as high as that in the minor peak (Figure 6D and E, respectively). Quantitative amino acid analyses of fractions from the reverse phase separation revealed the presence of 1 mol of propeptide and 2 mol of propeptide per enzyme dimer in the minor and the

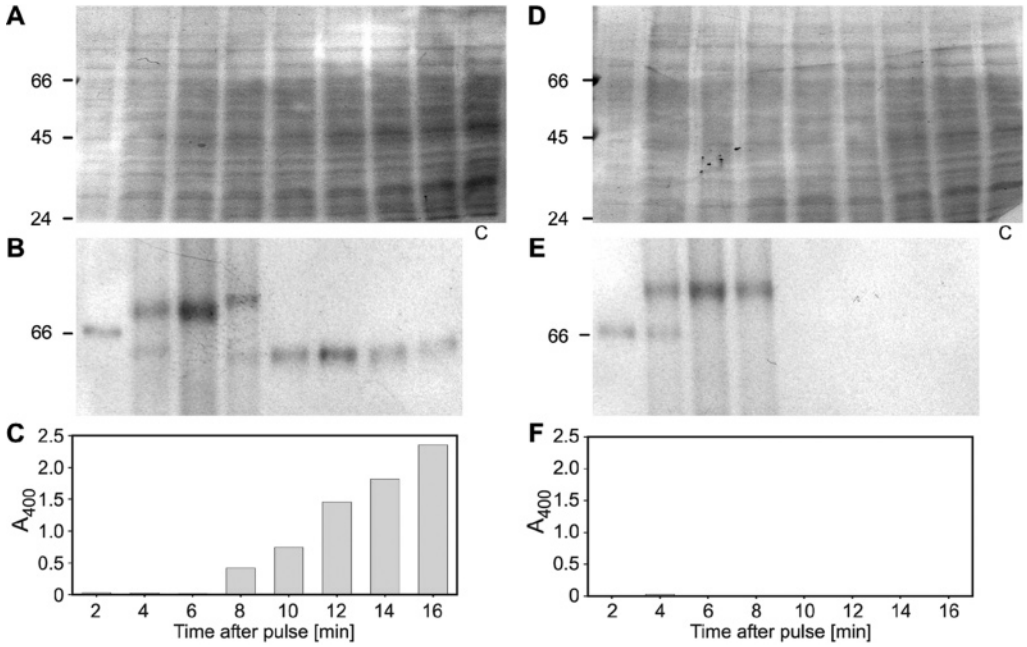

FIGURE 5: Effect of protease inhibitors, leupeptine (panels A−C), and Ser-Lys-Arg-CH_2-Cl (panels D−E) on the processing and activation of *A. oryzae* β-*N*-acetylhexosaminidase. (A and D) Total ^{35}[S] proteome of ER proteins examined by SDS−PAGE followed by fluorography. The control proteome from cells devoid of the inhibitors (C) is also indicated on the left. (B and E) Processing of the β-*N*-acetylhexosaminidase analyzed by the fluorography of the immunopurified ^{35}S-labeled enzyme. (C and F) Appearance of enzymatic activity measured by a colorimetric assay.

Table 1: Comparison of the Effects of Dibasic Peptidase Inhibitors on Hex Processing and on the Activity of Fugnal Kexins and Mammalian Prohormone-Converting Peptidases

		(% of control)					
compound	concn (mM)	Hex proc. *in vivo*	Hex proc. *in vitro*	Kex1p (ref 27 (*27*))	krp (ref 28 (*28*))	proinsulin endop.[a]	PC5 (ref 29 (*29*))
PMSF	10	101	98	<1	193	111.9	76
iodoacetic acid	1	6	7	n.d.	n.d.	109.2	n.d.
iodoacetamide	1	12	8	n.d.	n.d.	109.6	n.d.
N-ethylmaleiimide	1	20	23	n.d.	n.d.	98.5	n.d.
EDTA	6	114	105	99	n.d.	0	7
EGTA	6	106	112	77	n.d.	0	n.d.
1.10-phenantroline	6	99	100	n.d.	88	90	6
leupeptin	2	40	38	n.d.	104	62.1	n.d.
vanadate	0.1	113	102	n.d.	n.d.	113.8	n.d.
NaF	20	111	119	n.d.	n.d.	8.5	n.d.
$ZnCl_2$	1	96	98	7	20	9.3	n.d.
$HgCl_2$	0.05	105	106	2	0	0	2
Ala-Lys-Arg-CH_2Cl	0.1	58	45	n.d.	n.d.	4.6	n.d.
Ala-Arg-Arg-CH_2Cl	0.1	66	68	n.d.	n.d.	11.2	n.d.
Ser-Lys-Arg-CH_2Cl	0.1	4	3	n.d.	n.d.	n.d.	n.d.
Ser-Arg-Arg-CH_2Cl	0.1	13	15	n.d.	n.d.	n.d	n.d.

[a] Data were taken from ref 25 (*25*); n.d., not determined.

major peaks, respectively (data not shown). These data indicated that Hex was secreted exclusively as dimers in two different forms containing 1 or 2 mol of the propeptide per 2 mol of the catalytic subunits. The latter fully active form rich in propeptide was predominant in 48 h cultures.

An analogous separation of the intracellular enzyme disclosed the resolution of Hex into three components, two minor and one major (Figure 6F). Gel filtration analyses showed that although material in the first and in the last peaks contained dimeric Hex containing 1 and 2 mol of the propeptide, respectively, the intermediate peak contained the monomeric enzyme subunits (Figure 6G−I). Interestingly, although the monomeric enzyme subunits had very low enzyme activity, the dimeric enzyme in the first peak had only about half specific enzymatic activity when compared with that of the dimeric enzyme in the last peak (Figure 6G and I, respectively). Evaluation of the ratio propeptide/enzymatic subunit, performed in the same way as described for the secreted enzyme, revealed that the first peak was composed of the dimers associated with a single propeptide, and the last peak contained dimers with an equimolar amount of propeptide (two propeptides per enzyme dimer). There has also been a significant amount of propeptide present in the monomeric enzyme, corresponding to approximately 1 mol of propeptide per mole of the catalytic unit.

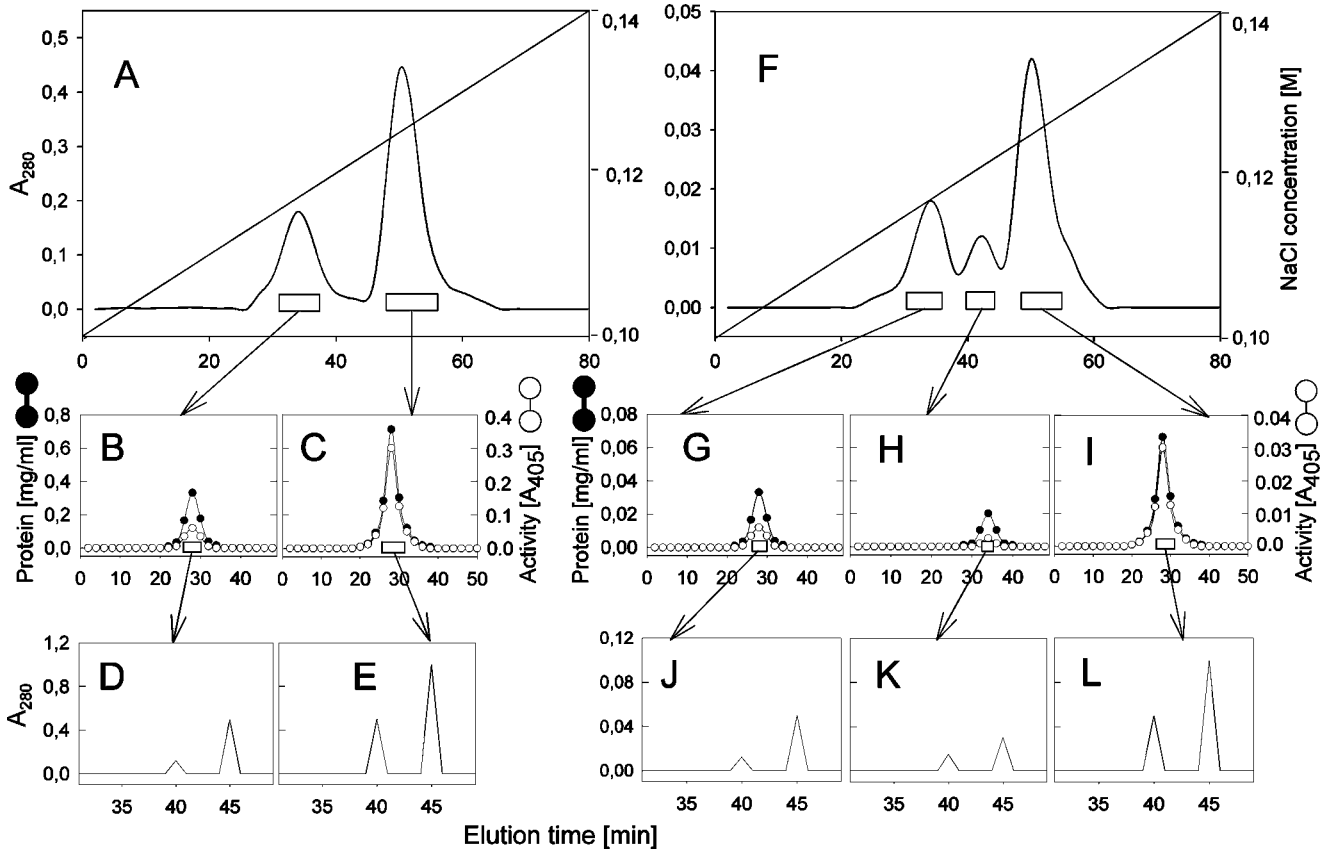

FIGURE 6: Molecular analysis of the extracellular form of *A. oryzae* β-*N*-acetylhexosaminidase by consecutive chromatography on MonoQ (A), followed by chromatography on Superdex 200 (B and C) and reverse phase separation using Vydac C-4 (D and E). The course of the analysis of the individual fractions is indicated by arrows. An intracellular form of the enzyme was analyzed by a similar sequence involving MonoQ chromatography (F), followed by Superdex 200 (G−I) and Vydac C-4 (J−L) separations.

Studies in Vitro of Hexosaminidase Processing, Activation, and Dimerization. In order to further evaluate the role of the propeptide in enzyme activation and the nature of the processing enzyme, we examined the unprocessed Hex polypeptide that could be immunoisolated as a minor fraction (less than 5%) from the mycelium of *A. oryzae*. As emphasized above, the unprocessed Hex seems to be unstable and is rapidly degraded within the cell. However, this enzyme can be isolated using rapid immunopurification and is moderately stable for at least several hours when kept at 4 °C. Upon heating to 28 °C, the standard cultivation temperature for *A. oryzae*, even the purified enzyme precipitates quantitatively in less than 1 h. Despite these technical difficulties, we could follow the *in vitro* processing of the enzyme upon its incubation with the detergent extract of the microsomal membranes at 18 °C, although the kinetics of enzyme processing (Figure 7A) and activation (Figure 7B) under these conditions was somewhat slower. Importantly, however, when we tested the effect of various inhibitors on the degree of enzyme processing under these conditions, we obtained results comparable to those obtained *in vivo* (Table 1).

Stability of the Enzyme in Vitro. From all of the above observations performed both *in vivo* and *in vitro*, it would appear that once the free propeptide is released, its association with the catalytic unit is rapid and very efficient resulting in the formation of a tight protein complex. Chemical conditions that are necessary to separate the propeptide from the catalytic subunit *in vitro* also point to a very strong interaction between the two components. Among the conditions worth mentioning are those applied during the reverse phase separation of Hex, involving the elution with acetonitrile up to 60% final concentration. When this separation is performed in an either neutral (ammonium acetate buffer

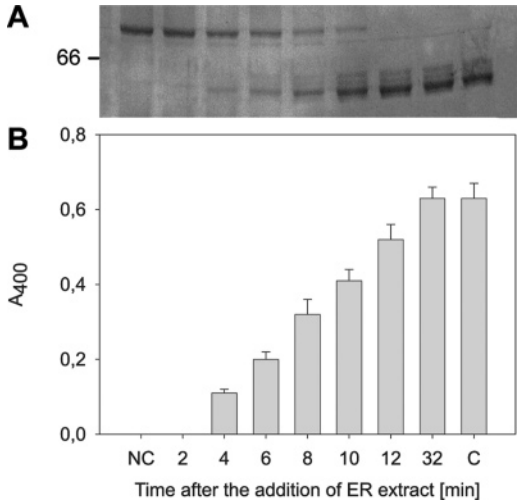

FIGURE 7: Processing of Hex by microsomal extract *in vitro*. (A) Time course of the processing examined by Western blotting using the polyclonal antibodies against catalytic subunit. The molecular marker is indicated on the left. (B) Time course of Hex activation followed by colorimetric measurement of enzyme activity. NC and C represent the nonprocessed and fully processed forms of Hex, respectively.

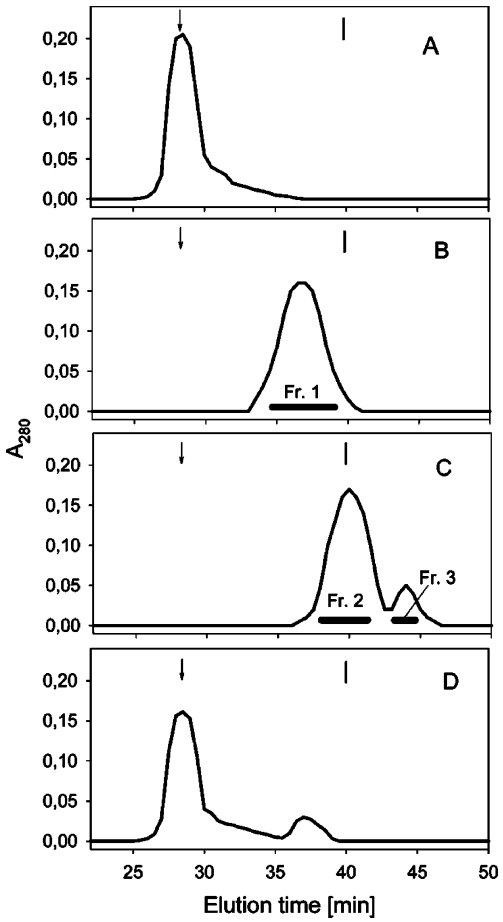

FIGURE 8: Analysis of the molecular architecture of *A. oryzae* β-*N*-acetylhexosaminidase by gel filtration on a Superdex 200 (10/30) column. (A) Fifty millimolar sodium citrate buffer at pH 3.5; (B) 50 mM sodium citrate buffer at pH 2.5; (C) 50 mM sodium citrate buffer at pH 2.5 with 20% acetonitrile; (D) reconstituted enzyme in 50 mM sodium citrate buffer at pH 5.0. Molecular mass markers include IgG (160 kDa, arrow) and BSA (65 kDa, vertical line). The void volume and the salt volume of the column were at 20 and 50 min, respectively. Fractions 1, 2, and 3 were collected as indicated and used for *in vitro* reconstitution experiments.

at pH 7.0) or mildly acidic (1% acetic acid pH 3.0) environment, Hex eluted as a single peak, retaining full enzymatic activity. Only the use of 0.1% TFA at pH 2.0 in combination with acetonitrile finally resulted in Hex dissociation and separate elution of the propeptide and the catalytic subunit in two peaks (*10*). In order to further investigate the details of Hex architecture under these extreme conditions, we systematically analyzed the enzyme by gel filtration on Superdex 200 in a series of buffers of gradually decreasing pH or in buffers containing acetonitrile. When Hex was subjected to gel permeation in buffers up to pH 3.5, it retained the original size of 160 kDa (Figure 8A), and the enzyme remained fully active after returning to the pH optimum (pH 5.0). However, when the enzyme was separated in citrate buffer at pH 2.5, the 160 kDa complex disappeared completely, yielding a smaller complex of approximately 80 kDa (Figure 8B). Quantitative evaluation of the N-terminal sequence from this material revealed an equimolar ratio of the catalytic subunit and the propeptide, which corresponded to one molecule of the catalytic subunit combined with one molecule of the propeptide. Moreover, significant enzymatic activity was retained by this 80 kDa complex. Only when the enzyme complex was incubated at pH 2.5 together with 20% acetonitrile did the propeptide dissociate from the catalytic subunit (Figure 8C). An identical result was obtained when the 80 kDa complex separated at pH 2.5 without acetonitrile and was concentrated and rechromatographed in the presence of 20% acetonitrile. When the isolated catalytic unit (Fraction 2 in Figure 8C) was returned to pH 5.0, no enzymatic activity was recovered. The addition of propeptide (Fraction 3 in Figure 8C) to such a preparation did not result in the restoration of any enzymatic activity even upon prolonged incubation at various temperatures, and the gradual aggregation of the catalytic subunit was observed after about 1 h. However, when the catalytic subunit was returned to pH 5.0 into a buffer already containing the propeptide, the enzymatic activity was readily ($t_{1/2} = 5$ min) restored concomitantly with the rapid formation of the 80 kDa complex. The formation of the original dimeric enzyme molecule has also been quite rapid, and once the 80 kDa complex had been formed, it proceeded with the kinetics identical to that recorded for this complex obtained in the absence of acetonitrile. Under these conditions, very little catalytic subunit or propeptide could be detected after 20 min of reconstitution (Figure 8D).

Although all the previous results indicate rapid and efficient interaction of the propeptide with the catalytic unit, the formation of enzyme dimers is somewhat slower. The summary of the data from the reconstitution experiments perfomed at 18 °C (in order to prevent the unfolded monomeric units from aggregation) are presented in Table 2. The half-time for the dimerization of Hex under these conditions seems to be about 10 min, and the lone catalytic subunit−propeptide pair has about 60% activity of the pair within the native dimer. Moreover, as we have reported previously (*10*), when the propeptide corresponding to only the half molar amount of the catalytic unit was added, the activity was restored to only half of the above specific activity, but the enzyme also formed a dimer, albeit with considerably slower kinetics ($t_{1/2} = 20$ min). Another interesting issue pertinent for the dimeric enzymes was the possible cooperativity between the two catalytic subunits. However, our detailed investigations of Hex kinetics found no evidence for this possibility with the values of the Hill's coefficient not significantly different from 1 (see the Hill's plot in Figure 2 of the Supporting Information), indicating that each catalytic subunit in the dimer works independently of the second subunit, albeit in close cooperation with its propeptide. Thus, three important conclusions could be drawn from the *in vitro* reconstitution experiments. First, the enzyme dimer can dissociate into monomers that still retain the propeptide bound to the catalytic subunit and full enzymatic activity. Second, the catalytic activity of Hex, its stability, and formation of the enzyme dimer are critically dependent on the presence of the propeptide. Third, the form of the enzyme consisting of two catalytic subunits combined with a single propeptide is still dimeric, but only the propeptide-paired catalytic subunit remains enzymatically active, and the kinetics of dimerization becomes somewhat slower.

Propeptide in the Endoplasmic Reticulum Regulates the Production of Active Hex Independent of the Rate of Transcription. An analysis of secreted Hex indicated that the enzyme in medium occurs as a mixture of dimers of the

Table 2: Analysis of the Efficiency of Reconstitution of *A. oryzae* β-*N*-Acetylhexosaminidase under Various Experimental Conditions[a]

			results of gel filtration (% of total protein in individual fractions)			
monomer 1	monomer 2	incubation	dimer	monomere +propeptide	monomer	relative activity (% of control)
fraction 1	none	10 min	54 ± 4	46 ± 3	n.d.	88
fraction 1	none	20 min	78 ± 2	22 ± 3	n.d.	90
fraction 1	none	60 min	98 ± 3	2 ± 1	n.d.	101
fraction 2	fraction 3	10 min	52 ± 4	44 ± 2	4 ± 1	86
fraction 2	fraction 3	20 min	79 ± 3.	21 ± 5	n.d.	91
fraction 2	fraction 3	60 min	98 ± 2	2 ± 1	n.d.	99

[a] The indicated fractions (Figure 8) were used as a source of monomeric enzyme subunits. These were mixed in 50 mM citrate buffer at pH 5.0, incubated at 18 °C for the indicated periods of time, and analyzed by rapid gel filtration as described in Materials and Methods. Individual fractions were quantified and expressed as the mean ± standard deviation from three independent experiments; n.d., not detectable.

catalytic subunit containing one or two molecules of the propeptide, the latter form of the enzyme having a 2-fold specific activity of that of the former. In order to understand the possible physiological relevance of this heterogeneity, we determined propeptide/catalytic subunit ratio in Hex produced by cultures at various stages of its growth. The accumulation of Hex in the culture fluid followed a typical biphasic curve (Figure 9A) with the first wave of production reaching a plateau between days 4 and 6 of culture, and the second wave of production peaking at day 10. Therefore, we have determined the propeptide/catalytic unit ratio during the exponential phase of the first wave (day 2), during the first plateau (days 4 and 6), during the second exponential phase (day 8), and during the second plateau (days 10 and 14). The summary of these data is shown in the Supporting Information Table 1. Overall, these analyses revealed dramatic differences in the propeptide/catalytic unit ratio, especially in the mycelium. Intracellularly, this ratio could span from 0.3 up to 2.0.

In order to understand the mechanisms of regulation of Hex under these conditions, we have followed the transcription of the *HexA* gene as well as the formation of Hex at the protein level. The level of transcription of the *HexA* gene did not differ significantly at individual stages of growth as indicated by the Northern blot analysis (Figure 9B). However, significant differences could be observed with regard to the molecular composition of Hex during these stages. During the exponential stage of growth, Hex was formed mostly in the form of highly active molecular species containing two molecules of the propeptide per enzyme dimer as revealed by molecular analysis of the enzyme isolated from the microsomes of the cultured fungus (Figure 9C, 2 days). In sharp contrast to these findings, the enzyme catalytic subunits immunoprecipitated from the stationary culture displayed an extremely low level of the associated propeptide (Figure 9C, 6 days). To further investigate the molecular mechanisms behind this unusual regulation, we assayed the levels of free propeptide in the endoplasmic reticulum (ER) and in the cytosol (CY) isolated from mycelium after varying periods of growth. The levels of free propeptide inside the ER were always very low, consistent with its efficient association with the enzyme catalytic subunits (Figure 9D). However, the levels of free propeptide in the cytosol were inversely proportional to its abundance on the Hex formed in the ER (Figure 9E). For instance, during the stationary culture at day 6 when the lowest level of Hex-associated and free propeptides were present in the ER, the highest level of the propeptide was present in the CY (Figure 9C, D, and E). These data strongly indicate that the fungus can regulate the free microsomal (ER) concentration of the propeptide by employing its active transport into the cytosol.

Propeptide Contents in Hex Significantly Influence the Rate of Intracellular Transport and Secretion. One interesting feature of the propeptide of Hex from *A. oryzae* revealed by the bioinformatic analysis was the identification of a total of six repetitions of a short peptide motif consisting of an acidic amino acid, a small side-chain amino acid, and a large hydrophobic amino acid, namely, sequences $Glu^{29}-Trp^{32}$, $Asp^{54}-Ile^{56}$, $Asp^{59}-Trp^{61}$, $Glu^{66}-Ile^{68}$, and $Glu^{86}-Phe^{88}$. These peptide repeats resembled the putative consensus sequence (Asp/Glu)(Gly/Pro)(Tyr/Phe), which was shown to be responsible for regulated secretion in plant glycoproteins (*30*). This indicated the possible role of the propeptide in the intracellular transport and secretion of Hex in addition to its other functions in enzyme activation and dimerization. To investigate this possible function of the propeptide, we made use of the naturally occurring Hex isoforms described above and measured the rate of secretion in 2 day exponential cultures, 4 day late log phase cultures, and 6 day stationary cultures in which the predominant form of intracellular Hex had propeptide/catalytic unit ratios of 2.0, 1.0, and 0.2, respectively (Figure 9C). Although the rate of intracellular Hex production was identical under all of these conditions (Figure 10A−C), the rate of Hex secretion defined as the slope of the curve monitoring its concentration in the medium was maximal in 2 day cultures and was very low in 6 day cultures (Figure 10A and C, respectively). Overall, the rate of Hex secretion correlated very well with its propeptide content (Figure 10D).

DISCUSSION

We describe here a novel mechanism that fungal hexosaminidases employ for the regulation of their enzymatic activity. This is based on the formation and secretion of two different forms of the enzyme molecules, one fully active and one half active. This mechanism is completely different from the allosteric regulation known for many enzymes regulating the key metabolic pathways. In allosteric enzymes, there is a continuous regulation of activity, depending on the concentration of the regulator, mediated by conformational change transferred from the regulatory to the catalytic

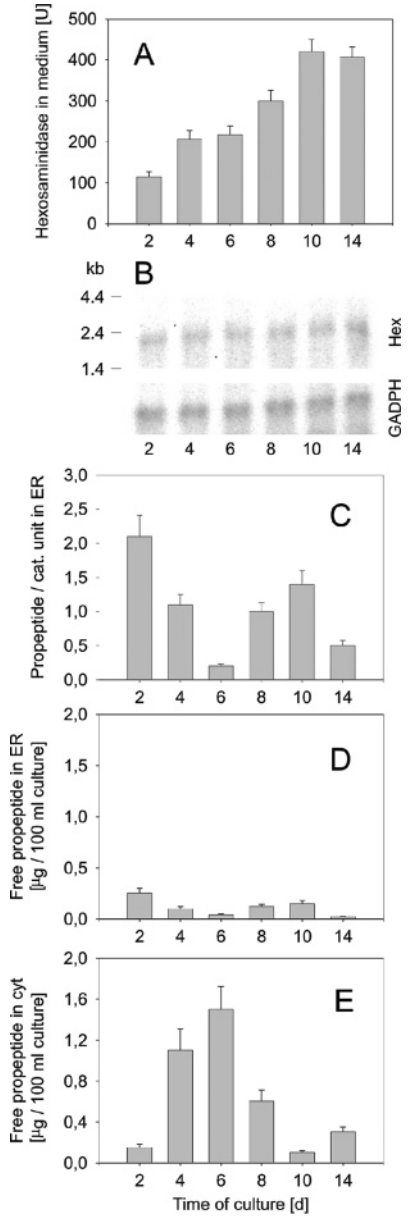

FIGURE 9: Propeptide of Hex regulates the activity of the enzyme during various stages of growth of the production fungus. (A) Accumulation of total Hex activity in the medium after several days of culture. Aliquots of the culture medium were withdrawn at the indicated times, and the result is from three cultivations with S.D. indicated by error bars. (B) Level of transcription of the *HexA* gene in *A. oryzae* assayed by Northern blot at the indicated times of culture and compared to GADPH transcription. (C) Ratio of the propeptide to catalytic units expressed as enzyme dimers in the ER in various days of culture. Hex was extracted from ER isolated from the mycelium after the indicated period of cultivation and immunopurified, and the ratio of the propeptide to the catalytic subunit was determined as described in Materials and Methods. The results are expressed as the means obtained from three independent cultivations with S.D. indicated by error bars. (D) and (E) Amount of free propeptide in ER and CY, respectively, assayed at the indicated days of culture. Hex was extracted from the ER and CY of mycelium cultivated for the indicated time, and the amount of free propeptide was determined after the immunodepletion of Hex by antibodies against the catalytic subunit using immunopurifications followed by HPLC and the determination of the propeptide by quantitative amino acid analyses as decribed in Materials and Methods. The results in panels D and E are the means from three independent cultivations with the S.D. indicated by error bars.

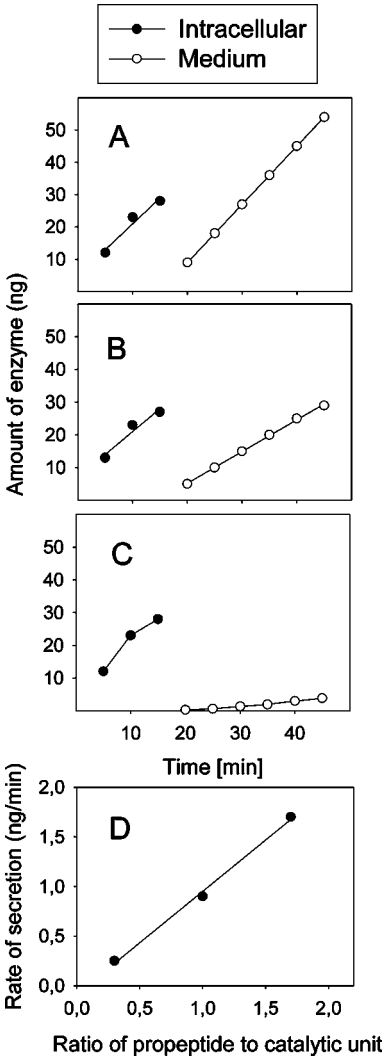

FIGURE 10: Rate of production of Hex and the rate of secretion at various times of the culture. The rate of Hex production and secretion was determined in cultures grown for 2 days (A), 4 days (B), and 6 days (C) by determining the amount of Hex in the mycelium and in the medium in aliquots withdrawn from short-term cultures after the indicated time of cultivation as described in Materials and Methods. (D) Rate of secretion determined as the slope of the secretion curve after 2, 4, and 6 days correlated with the propeptide/catalytic unit ratio taken from Figure 9C.

subunit. In contrast, an analysis of enzyme kinetics in fungal hexosaminidases did not reveal any cooperativity between the two catalytic subunits, and the propeptides that are critical for the regulation of enzymatic activity of catalytic subunits seem to do it in an on−off fashion.

Propeptide sequences have been shown previously to play various functions in the biosynthesis of lysosomal enzymes. In proteases, such as mouse cathepsin L, yeast carboxypeptidase Y, and subtilisin, they are necessary for the proper folding of the mature polypeptide (*31*). These propeptides were thus named Class I propeptides or intramolecular chaperones (*31*). They remain bound to the folded enzyme (either covalently or noncovalently), often inhibiting its activity. Eventually, they are released from the parent enzyme during its activation and degraded so that they may not be found in the mature enzymes. However, Class II propeptides are not directly involved in the catalysis of the folding reactions (*28*). Instead, they participate in a broad variety of other biological processes.

The results presented here indicate that the propeptides of fungal Hex keep them in the active state, which makes them different from other intramolecular chaperones reported to date. The only example of similar properties can be found in the propeptide of human Hex B, which was shown not to inhibit enzymatic activity. Moreover, this propeptide was not entirely degraded during maturation in the lysosomes (*24*). In this Hex, the propeptide remains covalently bound to the mature catalytic subunits by interchain disulfide bonds (*24*). However, the fungal hexosaminidases have developed their own unique mechanisms for propeptide association. First, there are essentially no cysteine residues in the propeptides of these hexosaminidases, precluding the above mechanism of covalent association, and here, we present evidence for noncovalent association. Second, although the fungal propeptides are bound noncovalently, their association with the catalytic subunits is very stable under physiological conditions for the entire life-span of the enzyme molecule. Third, the propeptide is not only very tightly bound to the catalytic subunit but also necessary for its catalytic function. In our reconstitution experiments, we were able to directly demonstrate the role of the propeptides of Hex from two filamentous fungi in the assembly of the native enzyme complex and in the establishment of enzymatic activity.

Although the processing of the Hex propeptide is an essential prerequisite for its folding, activation, and dimerization, it is difficult to speculate at this stage on the exact nature of the peptidase responsible for this processing. A large group of proprotein convertases specific for dibasic sequences has been identified in nearly all eukaryotic organisms including the filamentous fungi (*18*) forming a kexin subfamily of the eukaryotic subtilases (*32*). These enzymes are important in biotechnology for the production of recombinant proteins in filamentous fungi (*33*) but also play a role in the biology of this organism as evidenced by the lethality of the corresponding gene deletions (*28*). The known physiological substrates for kexin-like proteases in *A. niger* are the endopolygalacturonases that all contain a dibasic cleavage site at the carboxy-terminal end of their amino-terminal propeptide similar to that of Hex (*34*). However, our data indicate that the Hex-processing peptidase is most likely different from kexin-like dibasic peptidase on the basis of the differences in cellular location (ER vs late Golgi (*26*)), specificity, and the different patterns of reactions with the inhibitors. Our data point to the existence of a serine protease different from the fungal kexins and yapsins described (*35*), primarily localized in the ER. However, the exact molecular mechanism of catalysis by this processing peptidase as well the question of whether it is one processing enzyme with several substrate-binding pockets (*32*) or two separate enzymes will have to await further detailed molecular characterization. The data would indicate that the processing occurs co- or post-translationally early after N-glycosyaltion and signal peptide cleavage and most probably before the folding of the enzyme in ER.

Our results obtained both *in vitro* and *in vivo* allow us to draw some hypotheses about the key aspects of Hex folding and activation. The pulse−chase and inhibition data clearly indicate that the propeptide of Hex must be released from the rest of the polypeptide in order to be able to assist in enzyme activation. This behavior is unique and proceeds in a way opposite to that of the most studied Class I propeptides that mediate the folding of the polypeptide to which they remain covalently bound. Notably, it is this particular mechanism that allows the fungal cells to regulate the concentration of the propeptide independent of that of the catalytic unit. We hypothesize that by regulating the concentration of the free propeptide, the cell controls the amount and activity of secreted Hex depending on its metabolic needs. Thus, in the initial stage, when large activities of Hex are required for hyphal growth and remodeling, the enzyme is produced mostly in the form of fully active molecules. At the end of the log phase at day 4, when there is no longer such a high need for extracellular Hex, the production is switched mostly to half-active species. In the late stationary culture, very little Hex is produced altogether, which is connected with very low levels of both enzyme-associated and free propeptides in the ER. Later on, there is another shift toward the production of fully active enzyme molecules in the late stationary culture correlated with the need to increase again the activity of secreted Hex that is involved in the autolysis of the senescent dying cells. These data clearly indicate that the molecular form of Hex expressed during different stages of the cultivation of the producing organism is regulated by the availability of the propeptide in the ER. This mechanism reminds the assembly and peptide loading of class I and class II MHC antigens, during which the availability of the constituting polypeptides as well as the antigenic peptides inserted into the MHC peptide-presenting groove is essential (*36*, *37*). In the case of MHC class I, the peptide-loading protein complex has been shown to be composed of the peptide transporter TAP, glycoprotein tapasin, an ER chaperone calreticulin, and the thiol oxidoreductase Erp57 (*38*−*40*). In the case of MHC class II, the peptide exchange reaction leading to the binding of the external processed peptides in the endosomes depends on pH and is catalyzed by the HLA−DM protein complex (*41*). Although the chaperones and enzymes assisting in the binding of Hex propeptide to its catalytic subunit remain unclarified, the high efficiency of this association reaction compared to that of the formation of MHC peptide complexes, which are formed with an average efficiency of only 0.05%, is worth mentioning (*42*). This high efficiency is most probably due to the much larger size of the Hex propeptide. In view of this high efficiency of propeptide association with the catalytic subunit in Hex, we may assume that the formation of active Hex complexes in the ER of *Aspergillus* is very fast and that the formation of Hex molecules can be viewed as a competition between the catalytic subunit and the propeptide transporter for the molecule of the co- or post-translationally processed propeptide. In any case, the Hex results presented here represent the first example of this mechanism in the regulation of the activity of an enzyme.

In addition to the important role of the propeptide in Hex activation, we obtained evidence for its participation in other aspects of the life cycle of the enzyme. The most important among these functions are those related to enzyme dimerization and secretion. The most typical arrangement of Hex was shown to be formed by two noncovalently bound propeptides per enzyme dimer, and this form was found to be dominant in both the intracellular and the extracellular enzymes. Our data indicate that just one catalytic subunit paired with the propeptide can give rise to the enzyme dimer,

thus saving the lone catalytic subunit from destruction in the absence of the propeptide. However, the kinetics of binding of the propeptide to the catalytic subunit is faster than the formation of the dimer, and the two catalytic subunit/propeptide pairs seem to dimerize somewhat faster than the pair with one lone catalytic subunit. The participation of the propeptide in the secretion of Hex is especially interesting. Our results indicate that propeptide-free Hex molecules cannot be secreted. The good correlation between the propeptide content and secretion rate suggests another important regulatory mechanism that may work in accord with the propeptide-dependent enzyme activation. The Hex molecules that contain two propeptides per dimer of the catalytic units are not only more active than the half-charged species but also secreted faster. A combination of these two factors then provides the fungal cell with an additional possibility to regulate extracellular Hex activity over a broad range of values.

ACKNOWLEDGMENT

Dedicated to Professor Jan Kocourek on the occasion of his 80th birthday. We thank Dana Ulbrichová, Jiří Liberda, Přemysl Skočdopol, Petr Sedmera, and Iva Hrdličková for help with the experiments, Sylva Pažoutová, Miroslav Petříček, and Joachim Thiem for expert advice, and Jiří Ludvík for language corrections. We thank the reviewers for their valuable suggestions.

SUPPORTING INFORMATION AVAILABLE

Description of the isolation, sequencing, and cloning of hexosaminidases from *A. oryzae*, Figures describing the complete nucleotide and amino acid sequence of the *A. oryzae* enzyme, and a Table with the summary of analysis of secreted and intracellular hexosaminidases. This material is available free of charge via the Internet at http://pubs.acs.org.

REFERENCES

1. Weignerová, L., Vavrušková, P., Pišvejcová, A., Thiem, J., and Křen, V. (2003) Fungal *β-N*-acetylhexosaminidases with high *β-N*-acetylgalactosaminidase activity and their use for synthesis of *β*-GalNAc-containing oligosaccharides, *Carbohydr. Res. 338*, 1003−1008.
2. Korneluk, R. G., Mahuran, D. J., Noete, K., Klavins, M. H., O'Dowd, B. F., Tropak, M., Willard, H. F., Anderson, M. J., Lowden, J. A., and Gravel, R. A. (1986) Isolation of sDNA coding for the α-subunit of human *β*-hexosaminidase. Extensive homology between the α- and *β*-subunits and studies on Tay-Sachs disease, *J. Biol. Chem. 261*, 8407−8413.
3. Proia, R. L. (1988) Gene encoding the human *β*-hexosaminidase chain: extensive homology of intron placement in the α- and *β*-chain genes, *Proc. Natl. Acad. Sci. U.S.A. 85*, 1883−1887.
4. Tews, I., Perrakis, A., Oppenheim A., Dauter, Z., Wilson, K. S., and Vorgias, C. E. (1996) Bacterial chitobiase structure provides insight into catalytic mechanism and the basis of Tay-Sachs disease, *Nat. Struct. Biol. 3*, 638−648.
5. Huňková, Z., Křen, V., Ščigelová, M., Weignerová, L., Scheel, O., and Thiem, J. (1996) Induction of *β-N*-acetylhexosaminidases in *Aspergillus oryzae*, *Biotechnol. Lett. 18*, 725−730.
6. Huňková, Z., Kubátová, A., Weignerová, L., and Křen, V. (1999) Induction of extracellular glycosidases in filamentous fungi and their potential use in chemotaxonomy, *Czech. Mycol. 51*, 71−87.
7. Reyes, F., Calatayud, J., Vazquez, M. J., and Martinez, J. (1989) *β-N*-Acetylglucosaminidase from *Aspergillus nidulans* which degrades chitin oligomers during autolysis, *FEMS Microbiol. Lett. 53*, 83−87.
8. Gooday, G. W., Zhu, W.-Y., and O'Donell, R. W. (1992) What are the roles of chitinases in the growing fungus? *FEMS Microbiol. Lett. 100*, 387−392.
9. Peterbauer, C. K., Brunner, K., Mach, R. L., and Kubicek, C. P. (2002) Identification of the *N*-acetyl-D-glucosamine-inducible element in the promoter of the *Trichoderma atroviride nag1* gene encoding *N*-acetyl-glucosaminidase, *Mol. Genet. Genomics 267*, 162−167.
10. Plíhal, O., Sklenář, J., Kmoníčková, J., Man, P., Pompach, P., Havlíček, V., Křen, V., and Bezouška, K. (2004) N-Glycosylated catalytic unit meets O-glycosylated propeptide: complex protein architecture in a fungal hexosaminidase, *Biochem. Soc. Trans. 32*, 764−765.
11. Hušáková, L., Herkommerová-Rajnochová, E., Semeňuk, T., Kuzma, M., Rauvolfová, J., Přikrylová, V., Ettrich, R., Plíhal, O., Bezouška, K., and Křen, V. (2003) Enzymatic discrimination of 2-acetamido-2-deoxy-D-mannopyranose-containing disaccharides using *β-N*-acetylhexosa-minidases, *Adv. Synth. Catal. 345*, 735−742.
12. Angliker, H., Wikstrom, P., Shaw, E., Brenner, C., and Fuller, R. S. (1993) The synthesis of inhibitors for processing proteinases and their action on the Kex-2 proteinase of yeast. *Biochem. J. 293*, 75−81.
13. Altschul, S. F., and Lipman, D. J. (1990) Protein database searches for multiple alignments, *Proc. Natl. Acad. Sci. U.S.A. 87*, 5509−5513.
14. Harlow, E., and Lane, D. (1988) *Antibodies: A Laboratory Manual*, 2nd ed., pp 23−56, Cold Spring Harbor Laboratory, Cold Spring Harbor, NY.
15. Sambrook, J., Fritsch, E. F., and Maniatis, T. (1989) *Molecular Cloning: A Laboratory Manual*, 2nd ed., Cold Spring Harbor Laboratory, Cold Spring Harbor, NY.
16. Bezouška, K., Sklenář, J., Novák, P., Halada, P., Havlíček, V., Kraus, M., Tichá, M., and Jonáková, V. (1999) Determination of the complete covalent structure of the major glycoform of DQH sperm surface protein, a novel trypsin-resistant boar seminal plasma O-glycoprotein related to pB1 protein, *Protein Sci. 8*, 1551−1556.
17. Knapp, S., Vocadlo, D., Gao, Z., Kirk, B., Lou, J., and Withers, S. G. (1996) NAG-thiazoline, an *N*-acetyl-*β*-hexosaminidase inhibitor that implicates acetamido participation, *J. Am. Chem. Soc. 118*, 6804−6805.
18. Jalving, R., van de Vondervoort, P. J. I., Visser, J., and Schaap, P. J. (2000) Characterization of the kexin-like maturase of *Aspergillus niger*, *Appl. Environ. Microbiol. 66*, 363−368.
19. Li, Y. T., and Li, S. C. (1980) α-Mannosidase, *β-N*-acetylhexosaminidase and *β*-galactosidase from jack bean meal, *Methods Enzymol. 90*, 702−713.
20. Brumer, H., Sims, P. F. G., and Sinnott, M. L. (1999) Lignocellulose degradation by Phanerochaete chrysosporium: purification and characterization of the main α-galactosidase, *Biochem. J. 339*, 43−63.
21. Schagger, H. and Von Jagow, G. (1991) Blue native electrophoresis for isolation of membrane protein complexes in enzymatically active form, *Anal. Biochem. 199*, 223−231.
22. Machida, M., Asai, K., Sano, M., Tanaka, T., Kumagai, T., Terai, G, Kusumoto, K., Arima, T., Akita, O., Kashiwagi, Y., Abe, K., Gomi, K., Horiuchi, H., Kitamoto, K., Kobayashi, T., Takeuchi, M., Denning, D. W., Galagan, J. E., Nierman, W. C., Yu, J., Archer, D. B., Bennett, J. W., Bhatnagar, D., Cleveland, T. E., Fedorova, N. D., Gotoh, O., Horikawa, H., Hosoyama, A., Ichinomiya, M., Igarashi, R., Iwashita, K., Juvvadi, P. R., Kato, M., Kato, Y., Kin, T., Kokubun, A., Maeda, H., Maeyama, N., Maruyama, J., Nagasaki, H., Nakajima, ,T., Oda, K., Okada, K., Paulsen, I., Sakamoto, K., Sawano, T., Takahashi, M., Takase, K., Terabayashi, Y., Wortman, J. R., Yamada, O., Yamagata, Y., Anazawa, H., Hata, Y., Koide, Y., Komori, T., Koyama, Y., Minetoki, T., Suharnan, S., Tanaka, A., Isono, K., Kuhara, S., Ogasawara, N., and Kikuchi, H. (2005) Genome sequencing and analysis of *Aspergillus oryzae*, *Nature 438*, 1157−1161.
23. Diez, B., Rodriguez-Saiz, M., de la Fuente, J. L., Moreno, A. M., and Barredo, J. L. (2005) The *nagA* gene of *Penicillium chrysogenum* encoding *β*-N-acetylglucosaminidase, *FEMS Microbiol. Lett. 242*, 257−264.
24. Sagherian, C., Thorner, P., and Mahuran, D. (1994) The propeptide of the pro/b/polypeptide chain of human *β*-hexosaminidase is necessary for proper protein folding and exit from the

endoplasmic reticulum, *Biochem. Biophys. Res. Commun. 204*, 135−141.
25. Rhodes, C. J., Brennan, S. O., and Hutton, J. C. (1989) Proalbumin to albumin conversion by a proinsulin processing endopeptidase of insulin secretory granules, *J. Biol. Chem. 264*, 14240−14245.
26. Redding, K., Holcomb, C., and Fuller, R. S. (1991) Immunolocalization of Kex2 protease identifies a putative late Golgi compartment in the yeast *Saccharomyces cerevisiae*, *J. Cell Biol. 113*, 527−538.
27. Cooper, A., and Bussey, H. (1989) Characterization of the yeast *KEX1* gene product: a carboxypeptidase involved in processing secreted precursor proteins, *Mol. Cell. Biol. 9*, 2706−2714.
28. Davey, J., Davis, K., Imai, Y., Yamamoto, M., and Matthews, G. (1994) Isolation and characterization of krp, a dibasic endopeptidase required for cell viability in the fission yeast *Schizosaccharomyces pombe*, *EMBO J. 13*, 5910−5921.
29. Cain, B. M., Vishnuvardhan, D., Wang, W., Foulon, T., Cadel, S., Cohen, P., and Beinfeld, M. C. (2002) Production, purification and characterization of recombinant prohormone convertase 5 from baculovirus-infected insect cells, *Protein Expression Purif. 24*, 227−233.
30. Dal Degan, F., Child, R., Svendsen, I., and Ulvskov, P. (2001) The cleavable N-terminal domain of plant endopolygalacturonases from clade B may be involved in a regulated secretion mechanism, *J. Biol. Chem. 276*, 35297−35304.
31. Shinde, U., and Inouye, M. (2000) Intramolecular chaperones: polypeptide extensions that modulate protein folding, *Semin. Cell Dev. Biol. 11*, 35−44.
32. Siezen, R. J., and Leunissen, J. A. M. (1997) Subtilases: the superfamily of subtilisin-like proteases, *Protein Sci. 6*, 501−523.
33. Kjeldsen, T. (2000) Yeast secretory expression of insulin precursors, *Appl. Microbiol. Biotechnol. 54*, 277−286.
34. Jalving, R., van de Vondervoort, P. J. I., Visser, J., and Schaap, P. J. (2000) Characterization of the kexin-like maturase of *Aspergillus niger*, *Appl. Environ. Microbiol. 66*, 363−368.
35. Gagnon-Arsenault, I., Tremblay, J., and Bourbonnais, Y. (2006) Fungal yapsins and cell wall: a unique family of aspartic peptidases for a distinctive cellular function, *FEMS Yeast Res. 6*, 966−978.
36. Lehner, P. J., and Cresswell, P. (2004) Recent developments in MHC-class-I-mediated antigen presentation, *Curr. Opin. Immunol. 16*, 82−89.
37. Wubbolts, R., and Neefjes, J. (1999) Intracellular transport and peptide loading of MHC class II molecules: regulation by chaperones and motors, *Immunol. Rev. 172*, 189−208.
38. Cresswell, P., Bangia, N., Dick, T., and Diedrich, G. (1999) The nature of the MHC class I peptide loading complex, *Immunol. Rev. 172*, 21−28.
39. Sadasivan, B., Lehner, P. J., Ortmann, B., Spies, T., and Cresswell, P. (1996) Roles for calreticulin and a novel glycoprotein, tapasin, in the interaction of MHC class I molecules with TAP, *Immunity 5*, 103−114.
40. Hughes, E. A., and Cresswell, P. (1998) The thiol oxidoreductase Erp57 is a component of the MHC class I peptide-loading complex, *Curr. Biol. 8*, 709−712.
41. Jensen, P. E., Weber, D. A., Thayer, W. P., Westerman, L. E., and Dao, C. T. (1999) Peptide exchange in MHC molecules, *Immunol. Rev. 172*, 229−238.
42. Princiotta, M. F., Finzi, D., Qian, B. S., Gibbs, J., Schuchmann, S., Buttgereit, F., Bennink, J. R., and Yewdell, J. W. (2003) Quantitating protein synthesis, degradation, and endogenous antigen processing, *Immunity 18*, 343−354.

BI061828M